IEEE Access
Multidisciplinary | Rapid Review | Open Access Journal

Received 21 May 2025, accepted 3 June 2025, date of publication 9 June 2025, date of current version 16 June 2025.

Digital Object Identifier 10.1109/ACCESS.2025.3578248

RESEARCH ARTICLE

Advanced Fault Diagnosis in Milling Machines Using Acoustic Emission and Transfer Learning

MUHAMMAD UMAR[1], ZAHOOR AHMAD[1], SAIF ULLAH[1], FAISAL SALEEM[1], MUHAMMAD FAROOQ SIDDIQUE[1], AND JONG-MYON KIM[1,2], (Member, IEEE)

[1]Department of Electrical, Electronics, and Computer Engineering, University of Ulsan, Ulsan 44610, South Korea
[2]Prognosis and Diagnostics Technologies Company Ltd., Ulsan 44610, South Korea

Corresponding author: Jong-Myon Kim (jmkim07@ulsan.ac.kr)

This work was supported in part by the Technology Innovation Program (Development and Demonstration of Industrial IoT and AI-Based Process Facility Intelligence Support System in Small and Medium Manufacturing Sites) funded by the Ministry of Trade, Industry, and Energy (MOTIE, South Korea) under Grant 20023566; and in part by the Technology Innovation Program (The Development of Simulation Stage and Digital Twin for Land-Based Test Site and Hydrogen-Powered Vessel with Fuel Cell) funded by MOTIE under Grant RS-2022-00142509.

ABSTRACT The accurate diagnosis of faults in milling machines is important to ensure manufacturing efficiency and minimize downtime. Acoustic emission (AE) signals, known for their transient and high-frequency nature, provide valuable insights into tool and machine faults. However, their non-stationary characteristics present challenges for traditional analysis methods. This study proposes an innovative framework that combines time-frequency representation, transfer learning, and dimensionality reduction for effective fault diagnosis. AE signals are transformed into scalograms and spectrograms using continuous wavelet transform (CWT) and short-time Fourier transform (STFT), respectively, extracting both localized and global signal characteristics. These visual representations are processed through pre-trained deep learning architectures, EfficientNet-B0 and InceptionV3, to extract high-level features. Dimensionality reduction through uniform manifold approximation and projection (UMAP) further refines these features while preserving useful patterns. Finally, a lightweight k-nearest neighbors (k-NN) classifier is used to distinguish across all classes with high accuracy, achieving an average of 99.60% cross-validation performance. This framework highlights the strength of combining transfer learning with dimensionality reduction for fault diagnosis, providing a computationally efficient and highly accurate solution with significant potential for real-time monitoring and predictive maintenance in advanced manufacturing systems.

INDEX TERMS Acoustic emission, milling machine, fault diagnosis (FD), transfer learning, hybrid deep learning, uniform manifold approximation and projection.

I. INTRODUCTION

Milling machines are fundamental to modern industrial manufacturing, fulfilling important roles in sectors such as aerospace, automotive, and precision engineering [1]. These machines perform diverse tasks, including cutting, drilling, and shaping materials, often under demanding conditions characterized by high rotational speeds and significant loads. Such rigorous operating environments expose milling machines, especially their cutting tools, bearings, and gears, to frequent mechanical faults and wear [2]. Faults such as tool wear, bearing damage, and gear defects contribute greatly to machine breakdowns, with studies indicating that these issues account for more than 57% of mechanical failures in industrial settings [3]. These failures interrupt production lines, increase maintenance costs, and decrease overall productivity, impacting profitability. Timely and accurate fault diagnosis is essential for reducing machine downtime, improving operational reliability, and minimizing financial losses [4].

Over recent decades, there has been a shift toward the integration of advanced machine learning (ML) and deep learning (DL) techniques in condition monitoring systems, revolutionizing fault diagnosis approaches [5]. These technologies

The associate editor coordinating the review of this manuscript and approving it for publication was Guillermo Valencia-Palomo.

facilitate the early detection of faults, helping to prevent minor issues from leading to major malfunctions that can disrupt production [6]. While traditional condition-monitoring methods include direct visual inspections, which can be highly accurate, they are not feasible for real-time applications due to their disruptive nature and dependency on human expertise [7]. Indirect methods, using sensors to measure parameters like vibration and AE, have gained popularity due to their ability to continuously monitor machine health without interrupting operations [8]. AE monitoring has proven effective in detecting faults at their inception, offering an advantage over conventional vibration analysis by capturing high-frequency stress waves that reveal early mechanical issues [9]. Unlike vibration-based methods that may struggle with signal interpretation in complex environments, AE-based approaches can detect changes that indicate damage and are helpful for early-stage fault detection and predictive maintenance [10].

The introduction of time-frequency domain (TFD) analysis has significantly improved the detection of non-stationary signals in fault diagnosis applications [11]. Techniques such as CWT and STFT offer detailed time-frequency representations that capture transient signal characteristics and the development of these characteristics over time. CWT provides a high-resolution analysis that is particularly well-suited for observing localized changes in the signal, allowing the model to detect patterns that indicate wear or upcoming failure [12]. STFT, on the other hand, offers a consistent time-frequency resolution that is valuable for analyzing steady-state phenomena. These methods allow a deeper understanding of the temporal evolution of faults, allowing the detection and classification of complex machine conditions [13]. Previous studies have shown the effectiveness of combining TFD with DL architectures, such as convolutional neural networks (CNNs), to automate feature extraction and enhance the accuracy of fault detection models. CNNs, with their ability to learn hierarchical features, excel in transforming TFD outputs into representations that capture both global and localized fault patterns [14]. However, single model approaches often fail to handle overlapping fault classes and generalize across machine conditions. Challenges like overfitting specific faults and difficulty distinguishing closely related classes still impact fault diagnosis accuracy and robustness [15]. Another major challenge is the effective extraction and utilization of features from multi-domain data [16]. While CWT and STFT provide comprehensive time-frequency information, the sheer volume and high dimensionality of these features can make it difficult for models to process and classify them effectively. High-dimensional data increases computational load and can introduce redundancy, which can degrade model performance [17]. Moreover, traditional feature extraction methods may not adequately capture the intricate, small changes in the patterns needed for distinguishing between similar fault types or overlapping fault conditions. This can lead to reduced classification performance and increased computational overhead, hindering real-time implementation [18]. Noise interference and irrelevant features further complicate diagnosis, as they can obscure meaningful data and reduce model reliability [19].

A. RELATED LITERATURE

AE signals arise from the release of elastic energy due to material deformation or fractures, detected as AE hits by specialized sensors. Faults in milling machines alter AE signal distribution, making them valuable for condition monitoring [20]. Researchers extract fault-related features from AE signals in time, frequency, and time-frequency domains. These indicators are then analyzed using AI methods for fault classification and diagnosis. For instance, Twardowski et al. [21] utilized a temporal domain indicator, such as RMS, extracted from specific frequency bands and classified using a decision tree to monitor tool conditions. Similarly, Medina et al. [22] applied random forest classifiers to AE Poincaré plots to identify defects like broken teeth, pitting, scuffing, and cracks in gears. Li et al. [23] combined long short-term memory networks with support vector data to detect wear conditions from one-dimensional time-domain signals.

The presence of faults changes the frequency spectrum of AE signals, allowing the use of spectral domain analysis for the assessment of machine health. Bai [24] introduced a lightweight deep learning model that utilized statistical time domain and frequency domain indicators, such as mean, RMS, variance, and mean frequency, to diagnose faults in computerized numeric control (CNC) electromechanical systems. Despite the success of these methods, several challenges remain. For example, time-domain indicators can be affected by noise, decreasing their reliability for diagnosing complex faults. Similarly, while frequency domain methods are effective for stationary signals, the non-stationary nature of AE signals in milling operations often reduces their accuracy. To address this, modern TFD techniques, including wavelet transform, empirical mode decomposition (EMD), and variational mode decomposition, have been used to extract detailed fault-related information [25].

Faults in milling machine components release elastic energy, detected as AE hits by sensors. These hits provide key features such as peak amplitude, hit counts, rise time, decay time, and average frequency, independent of the overall AE signal distribution. These features are useful in structural monitoring and rotating machinery diagnostics, providing key insights into machine conditions. However, AE signals often contain noise from vibrations, tool interactions, and environmental factors, making fault detection challenging [26]. Deep learning performs better than traditional methods by automating feature extraction, eliminating manual engineering. Models like CNNs, LSTMs, and deep belief networks have shown effectiveness in fault diagnosis [27]. CNNs excel at extracting spatial features using

shared weights and local receptive fields, which reduce computational demands and the risk of overfitting. These networks have achieved notable success in diagnosing faults in bearings, gears, and cutting tools [28]. However, while CNNs are efficient for spatial feature extraction, they are less adept at capturing temporal dependencies inherent in sequential data, such as AE signals. This limitation highlights the need for methods that integrate both spatial and temporal features for more accurate fault diagnosis in complex systems like milling machines.

To address these challenges, this study proposes an innovative framework that integrates time-frequency representation, transfer learning, and dimensionality reduction for fault diagnosis in milling machines. AE signals are first transformed into scalograms and spectrograms using CWT and STFT, capturing both localized and global characteristics of the signal. These visual representations are then processed using EfficientNet and InceptionV3, two state-of-the-art pre-trained deep learning architectures known for their ability to extract meaningful and discriminative features. Transfer learning enables the use of pre-trained weights from large datasets, significantly enhancing feature extraction from scalogram and spectrogram representations while reducing the need for extensive labeled data. To further optimize the computational efficiency and effectiveness of the framework, UMAP is applied for dimensionality reduction. UMAP preserves the intrinsic structure of the data while minimizing feature redundancy, ensuring that only the most relevant information is retained for classification. The final step in the proposed framework uses a k-NN classifier to distinguish between all classes. The proposed approach achieves high cross-validation accuracy, proving its effectiveness in diagnosing faults across various conditions. By integrating transfer learning and dimensionality reduction, it enhances computational efficiency, making it ideal for real-time monitoring and predictive maintenance. The key novelties and contributions are as follows.

1. A novel hybrid framework integrates CWT and STFT representations to capture both localized and global time-frequency signal characteristics, enhancing fault diagnosis in milling machines.
2. Transfer learning is applied using pre-trained EfficientNet-B0 and InceptionV3 architectures, enabling high-level feature extraction from AE scalograms and spectrograms.
3. UMAP is applied for dimensionality reduction, optimizing computational efficiency while preserving the key patterns necessary for fault classification.
4. The k-NN classifier is used for fault classification, ensuring simplicity and effectiveness.
5. The proposed approach is validated using real-world AE data collected from a controlled laboratory milling machine testbed, demonstrating its effectiveness in detecting various operating conditions accurately.

The remaining paper is structured as follows: Section II outlines the technical concepts underpinning the proposed methodology, while Section III details the experimental setup and data acquisition process and discusses the results and comparative analysis, followed by conclusions and future recommendations in Section IV.

II. PROPOSED METHOD

This method detects milling machine faults by analyzing AE signals using time-frequency analysis, transfer learning-based feature extraction, dimensionality reduction, and classification. It integrates CWT scalograms and STFT spectrograms to capture key patterns, employing EfficientNet, InceptionV3, UMAP, and k-NN for fault classification. The complete workflow, shown in Figure 1, follows these steps.

Step 1: AE signals collected from the milling process originate from various mechanical interactions, i.e., chip formation, friction, tool wear, and material deformation. These interactions generate distinct transient bursts and frequency variations, which encode critical fault information. However, baseline fluctuations in raw AE signals can obscure these meaningful patterns, making fault interpretation challenging. To ensure that the extracted features accurately reflect fault-related variations, we apply mean removal, which eliminates signal offsets while preserving essential AE characteristics.

Step 2: To further enhance interpretability, we perform time-frequency transformation using CWT generates scalograms that highlight localized signal variations, capturing the short-term transient bursts caused by sudden tool breakage, gear impact, and abrupt material deformation. STFT produces spectrograms that reveal global frequency evolution over time, which is useful for identifying progressive tool wear, bearing degradation, and periodic fault signatures.

Step 3: Features are extracted from scalograms and spectrograms using pre-trained EfficientNet and InceptionV3 models. EfficientNet focuses on localized patterns in scalograms, while InceptionV3 captures both fine details and overall trends in spectrograms. Pre-trained on ImageNet, these models act as feature extractors with their final classification layers removed to focus solely on pattern identification.

Step 4: The extracted features from both models are high-dimensional and computationally expensive to process directly. UMAP is applied to reduce the dimensionality of the extracted features. For the STFT features, the dimensionality is reduced from 2048 to 50, while those for the CWT features are reduced from 1280 to 50. This ensures that the data remains compact and computationally efficient while retaining essential information.

Step 5: The reduced features from the two datasets are combined into a single set of feature pool of 100 features, 50 from STFT and 50 from CWT. Combining these features ensures that local and global patterns in the AE signals are used for classification.

Step 6: The combined features are classified using the k-NN algorithm, with $k = 5$ and Euclidean distance as the metric. The classifier achieved an average accuracy of

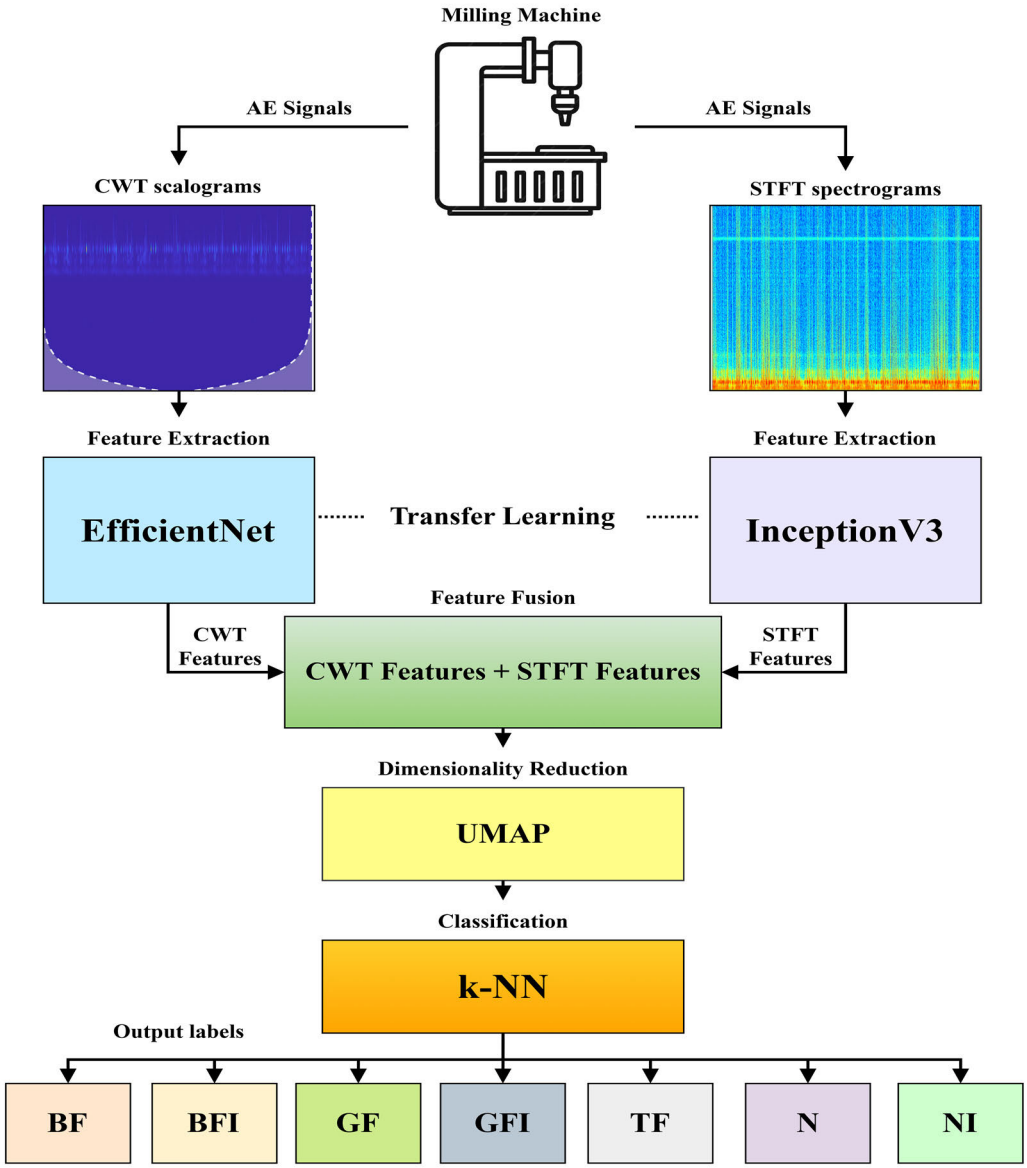

FIGURE 1. Workflow of the proposed method for fault diagnosis in milling machines.

99.60% during cross-validation, showing its effectiveness in distinguishing between all classes.

A. CONTINUOUS WAVELET TRANSFORM

CWT is a key technique for analyzing non-stationary signals, offering localized time-frequency representations. Unlike the Fourier Transform, it captures transient events in AE signals, making it ideal for fault diagnosis. The CWT decomposes a signal into a set of wavelet coefficients by convolving it with a scaled and shifted version of a mother wavelet. It provides a time-scale representation, converted into a time-frequency representation through scale-frequency relationships. Figure 2 shows CWT scalograms offering detailed time-frequency insights into AE signals used in the current study, which are high-frequency, transient, and non-stationary. Applied to AE signals from the milling process, CWT generates scalograms reflecting operational variations.

B. SHORT-TIME FOURIER TRANSFORM

STFT is a key signal processing technique that visualizes spectral energy changes over time. By segmenting the signal overlapping windows and applying the Fourier Transform, it captures transient and time-varying features, producing a time-frequency representation called a spectrogram [30]. This is vital for analyzing AE signals with high-frequency bursts from micro-cracks or cutting process changes. Shorter windows capture quick temporal changes, while longer ones enhance frequency precision. STFT transforms AE signals

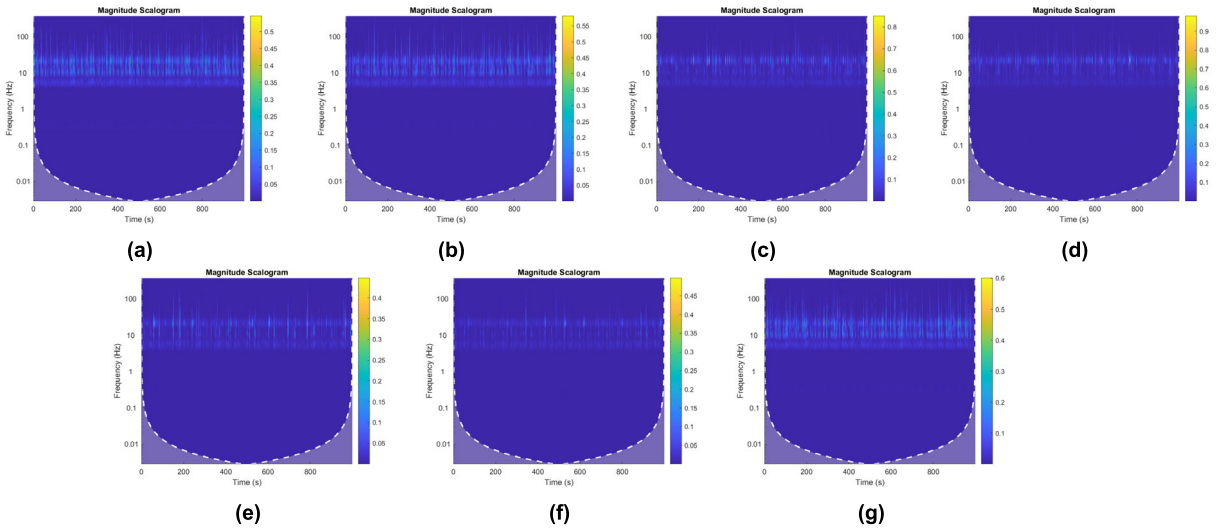

FIGURE 2. CWT scalograms: (a) N; (b) NI; (c) BF; (d) BFI; (e) GF; (f) GFI; and (g) TF.

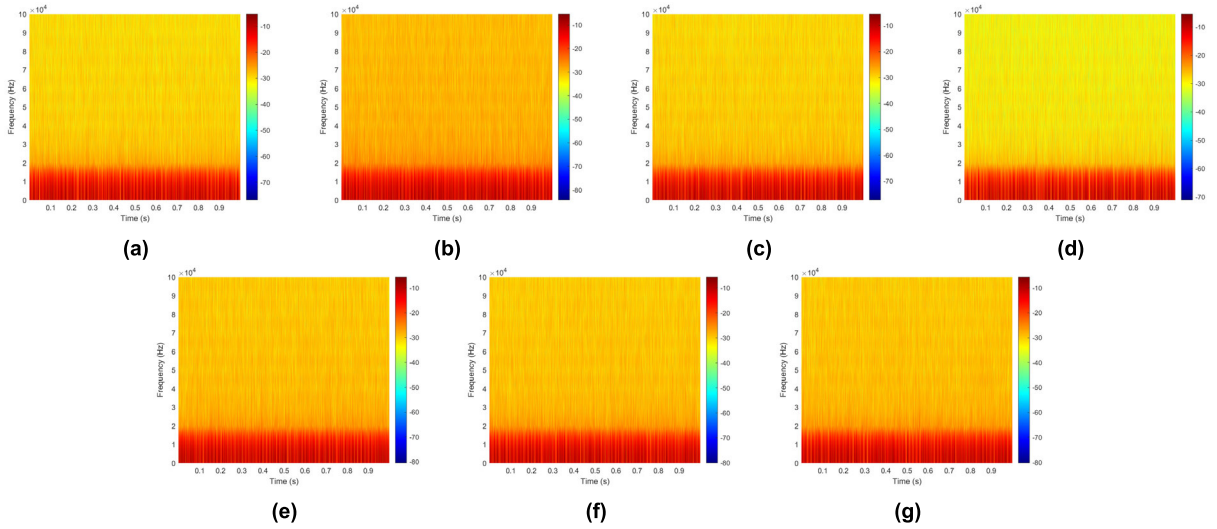

FIGURE 3. STFT spectrograms: (a) N; (b) NI; (c) BF; (d) BFI; (e) GF; (f) GFI; and (g) TF.

into spectrograms, serving as input features for deep learning, as shown in Figure 3, which visualizes spectral energy evolution over time.

C. TRANSFER LEARNING

Transfer learning reuses knowledge from models trained on large datasets to solve tasks in domains with limited labeled data. It is particularly useful when collecting and labeling domain-specific data is challenging. By utilizing pre-trained models, it reduces computational cost, training time, and enhances performance [32]. This study uses EfficientNet and InceptionV3 as pre-trained models to extract high-level features from scalograms and spectrograms, as shown in Figure 4, highlighting their ability to capture discriminative features.

1) EfficientNet-B0

EfficientNet is a family of deep neural networks that balance accuracy and computational efficiency using compound scaling to scale network dimensions. The EfficientNet-B0 architecture, pre-trained on ImageNet, is adapted to process 224×224 resized CWT scalograms, which capture localized time-frequency information. The pre-trained layers extract hierarchical features, while the fully connected layer is.

2) InceptionV3

InceptionV3 is a deep convolutional neural network that uses innovative architectural designs, such as inception modules, which apply multiple filter sizes in parallel to extract features at different spatial scales, as in Figure 6. This multi-scale feature extraction capability makes the model highly effective

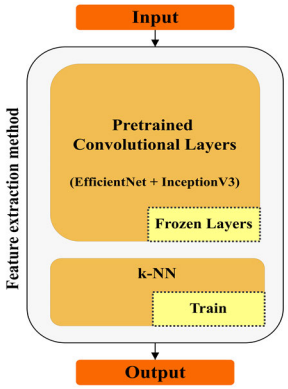

FIGURE 4. Feature extraction through transfer learning.

TABLE 1. Training parameters of the pre-trained models.

Parameter	EfficientNet-B0	InceptionV3
Number of Layers	82	48
Total Parameters	5.3 million	23.9 million
Input Size	224 × 224	229 × 229
Dropout Rate	0.2	0.4
Feature Vector Size	1280	2048
Pre-trained Dataset	ImageNet	ImageNet
Learning Rate	0.016	0.016
Optimizer Used	RMSProp	RMSProp

for analyzing complex patterns in visual data. Pre-trained on ImageNet, InceptionV3 excels in generalization and adapts well to domain-specific tasks with limited labeled data. In this approach, it is adapted to process STFT spectrograms from AE signals, resized to 229 × 229 pixels for input. The pre-trained convolutional layers extract high-level features, with the final fully connected layer replaced by an identity map for feature extraction. The framework leverages EfficientNet for localized features from scalograms and InceptionV3 for multi-scale patterns in spectrograms. These complementary features are fused into a unified space for accurate fault state classification. Transfer learning ensures the methodology benefits from pre-trained expertise while adapting to AE signal analysis. This combination enhances accuracy, scalability, and efficiency, with architectural and training parameters summarized in Table 1.

D. UNIFORM MANIFOLD APPROXIMATION AND PROJECTION

UMAP is a powerful method for reducing high-dimensional data while preserving its structure. It is particularly effective for simplifying complex datasets, like the features from scalograms and spectrograms. This reduces the computational burden of large feature sets and enhances classification model performance [31]. In this study, UMAP was applied to features from EfficientNet and InceptionV3, reducing the original sizes (2048 for STFT and 1280 for CWT) to 50 features each. Table 2 shows it preserved 98.7% and 99.5% of the variance for CWT and STFT, respectively, while significantly improving computational efficiency.

TABLE 2. Feature extraction statistics.

Model	Original Dimensions	Reduced Dimensions	Variance (%)
CWT (EfficientNet)	1280	50	98.7
STFT (InceptionV3)	2048	50	99.5

TABLE 3. UMAP parameters for dimensionality reduction.

n_components	metrics	n_neighbors	min_dist	random_state
50	Euclidean	15	0.1	42

TABLE 4. k-NN parameters for classification.

Parameters	Values
n_neigbhors	[5,10,15,20,25]
weights	[‘uniform’, ‘distance’]
algorithm	[‘auto’, ‘ball_tree’, ‘kd_tree’, ‘brute’]
leaf_size	[30, 40, 50]
p	[1,2]

To determine the optimal UMAP parameters, we conducted an iterative grid search, evaluating different values for n_neighbors and min_dist to maximize fault category separation while preventing overfitting. This dimensionality reduction improved the efficiency of the proposed framework. UMAP constructs a graph in the original high-dimensional space, maintaining point distances, and optimizes it in a low-dimensional space, preserving both local structures and cluster separation. The parameters used, detailed in Table 3, demonstrate how UMAP was configured to streamline the extracted features.

E. k-NEAREST NEIGHBOR

The k-NN algorithm is a simple and effective method for classifying data. It works by finding the closest k neighbors to a given data point in the feature space and assigning the label based on the majority class of those neighbors. The distance between points is usually calculated using metrics like Euclidean or Manhattan distance [31]. This algorithm is effective for complex datasets as it avoids data distribution assumptions, handles multiple classes, and utilizes local patterns for decision-making. Its simplicity makes it ideal for high-dimensional data with local patterns. The reduced STFT and CWT features are combined into a compact, unified set, serving as input to the classifier. The classifier is trained and tested on this combined dataset to evaluate performance. To select the optimal k value, we performed cross-validation on the training set, testing values between 1 and 20. The best-performing configuration was found to be $k = 5$ with Euclidean distance, which provided the highest classification accuracy while avoiding sensitivity to noise.

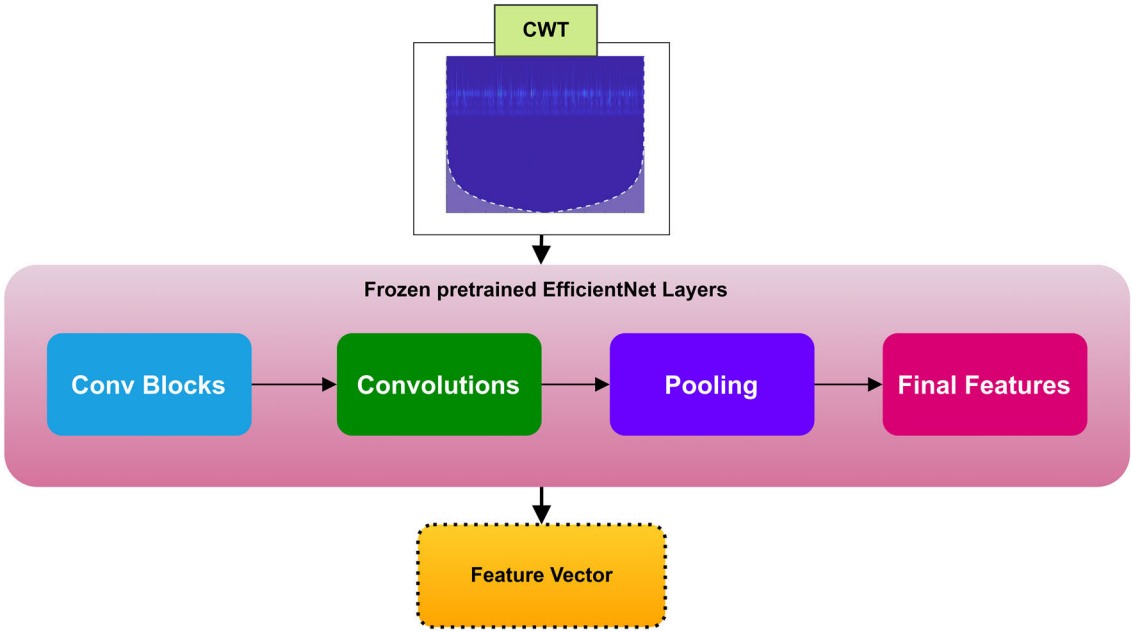

FIGURE 5. Feature extraction from CWT scalograms using EfficientNet.

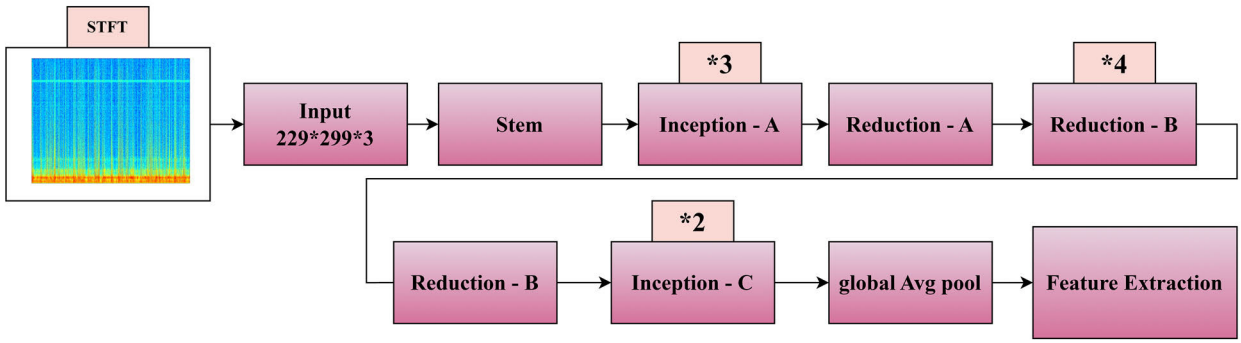

FIGURE 6. InceptionV3 architecture for feature extraction from STFT spectrograms.

Table 4 outlines the optimized parameters, enhancing fault classification performance.

III. RESULTS AND DISCUSSION

The effectiveness of the proposed method is assessed using AE data obtained from an actual milling machine. Since the primary aim of this method is to detect and diagnose faults in milling machines, this section begins by comparing the fault detection capability of the proposed method with existing time-domain indicators. Subsequently, the method's performance in fault classification is evaluated against other current approaches.

A. EXPERIMENTAL SETUP AND DATA ACQUISITION

AE signals were collected from a milling machine during controlled experiments to monitor and analyze fault conditions; the experimental setup is shown in Fig. 7. The milling operations were conducted on an INTER-SIEG X1 Micro Mill Drill, constructed from cast iron and resembling a small-scale pillar drill. This machine was used to perform straight parallel milling operations on steel workpieces. These operations are commonly used in shaping and machining hard materials. The cutting tool was a 2-flute carbide end mill intentionally worn to an average flank wear of 0.3 mm, as recommended by ISO-8688-2 standards for tool lifespan. The machine was carried out under control conditions, with the motor operating at 1320 RPM with 22 Hz frequency, the spindle at 660 RPM with 11 Hz frequency, and a bed feed rate of 0.4 mm/s. These stable parameters ensured consistent AE signal generation and captured distinct fault signatures. The steel workpieces, each measuring 20 mm $\times$ 35 mm $\times$ 35 mm, were processed in the experiment, with examples of unprocessed and processed samples shown in Figures 8 (a) and 8 (b), respectively.

To enhance the data quality, two AE sensors (R15I-AST, MISTRAS, Inc., USA) were employed. The primary sensor was mounted on the spindle to monitor signals associated with tool, bearing, and gear conditions. The secondary sensor

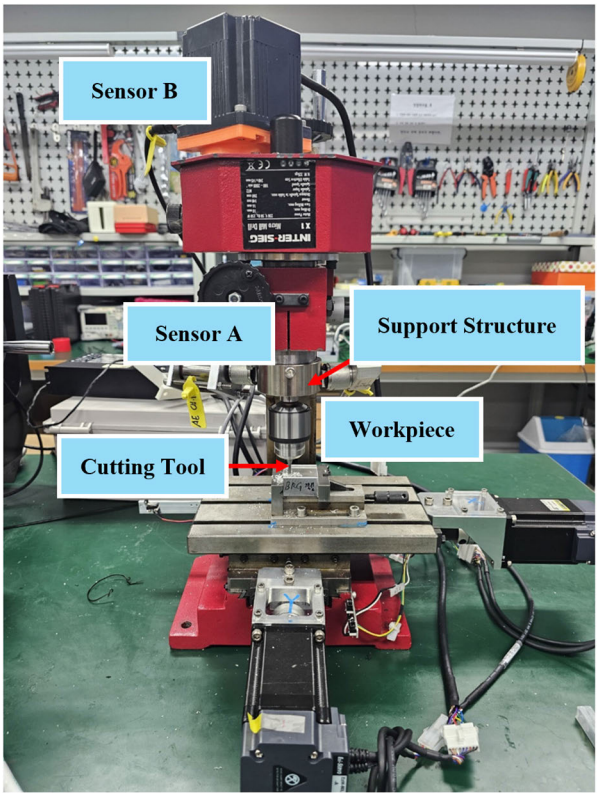

FIGURE 7. Experimental setup of a milling machine.

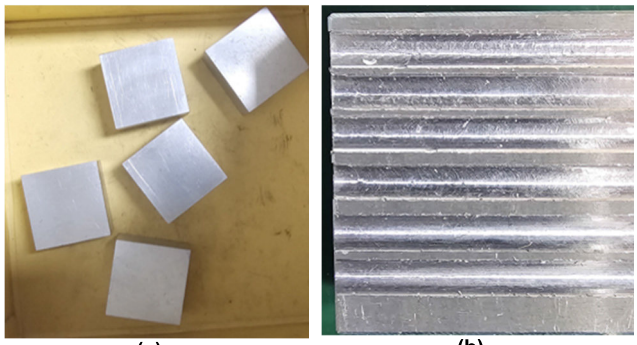

FIGURE 8. Workpieces for data collection: (a) Unprocessed; (b) Processed workpiece.

was affixed to the motor, functioning as a guard transducer to filter out irrelevant signals and noise. Both sensors were secured with industrial-grade adhesives to maintain stable and accurate signal acquisition throughout the experiments. The functionality of the sensors was validated using the HSU-Nelson test, which confirmed their ability to detect AE events effectively. AE signals were captured using the NI-9223 data acquisition system from National Instruments. Data acquisition was performed at a high sampling frequency of 1 MHz, ensuring the capture of transient and high-frequency bursts characteristic of the AE signals. A bandpass filter was applied to eliminate low-frequency noise and high-frequency interference, improving the overall signal quality for subsequent analysis. Data from the two sensors were synchronized,

TABLE 5. Summary of collected data operating conditions.

Operational Conditions	Number of Samples	Sampling rate	Collection Time
Normal (N)	40	1 MHz	2 minutes
Normal Idle (NI)	40	1 MHz	2 minutes
Bearing Fault (BF)	40	1 MHz	2 minutes
Bearing Fault Idle (BFI)	40	1 MHz	2 minutes
Gear Fault (GF)	40	1 MHz	2 minutes
Gear Fault Idle (GFI)	40	1 MHz	2 minutes
Tool Fault (TF)	40	1 MHz	2 minutes

TABLE 6. Comprehensive overview of the experimental setup.

Parameters	Specifications
Machine Model	INTER-SIEG X1 Micro Mill Drill
Spindle Speed	660 RPM (11 Hz)
Motor Speed	1320 RPM (22 Hz)
Cutting depth	2 mm
Bed Feed Rate	0.4 mm/s (for cutting conditions)
Sensors	Motor: 100 mV/g, Chuck: 500 mV/g
Workpiece Dimensions	20 mm × 35 mm × 35 mm
Operating Conditions	Idle and cutting
Fault Types	Tool Fault (1-2 mm blade breakage), Bearing Fault (3 mm depth), Gear Fault (2-3 mm depth, 1.5 mm width)

enabling time-aligned comparisons of fault conditions across components of the milling machine. The machine was placed on a base equipped with shock absorbers to reduce mechanical vibrations that could interfere with AE signal acquisition. AE sensors were placed in an acoustically shielded environment, with surrounding vibration-damping materials to minimize background noise. The experimental setup was in a controlled laboratory environment, isolated from external mechanical noise sources such as other running machines.

To simulate various fault conditions, intentional defects were introduced into the milling machine components. For the tool fault condition, the cutting tool was worn to an average flank wear of 0.3 mm. In the bearing fault condition, a defect was created in the outer race of the bearing supporting the tool. For the gear fault condition, a small fragment was removed from one of the gear teeth, transmitting torque from the motor to the spindle. Each fault condition generated distinct transient patterns in the AE signals, critical for fault classification. Signals were recorded under both idle and cutting operations. A total of 40 samples were collected for each operating condition, resulting in a comprehensive dataset of 280 samples, as summarized in Table 5. The experimental platform included shafts with 16-tooth, 32-tooth, and 30-tooth gears, with the spindle connected to the 30-tooth gear shaft. Faults were created through laser processing and impact methods, resulting in defects of 3 mm depth, gear faults with tooth damage, and tool blade breakages. These faults were systematically introduced and validated using time-domain and frequency-domain analysis. Figures 9, 11, and 12 illustrate the AE time-domain signals, AE frequency-domain signals, and the faulty components used in the experiments, respectively.

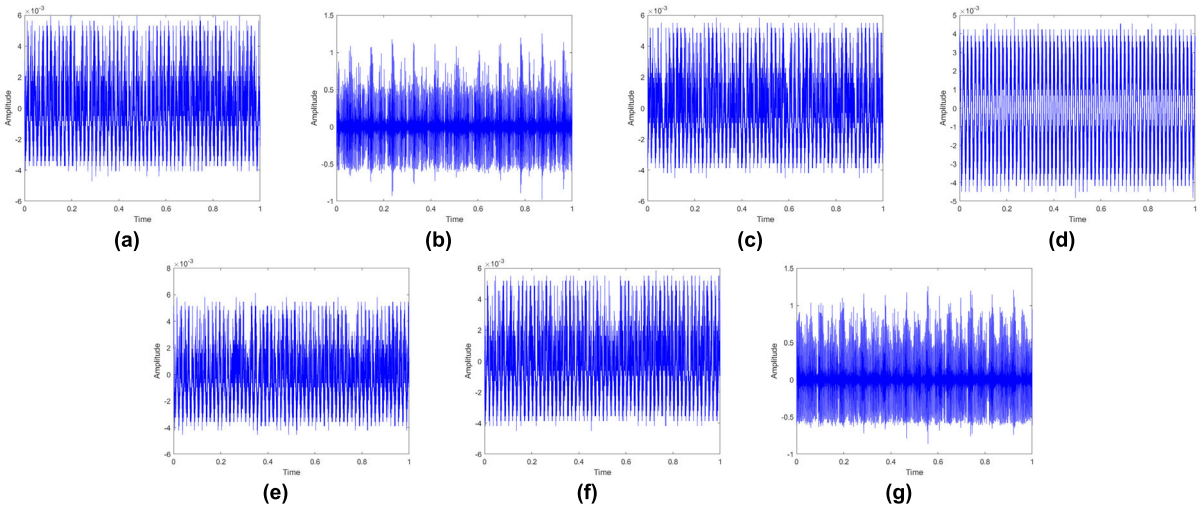

FIGURE 9. AE time domain signals (a) N; (b) NI; (c) BF; (d) BFI; (e) GF; (f) GFI; and (g) TF.

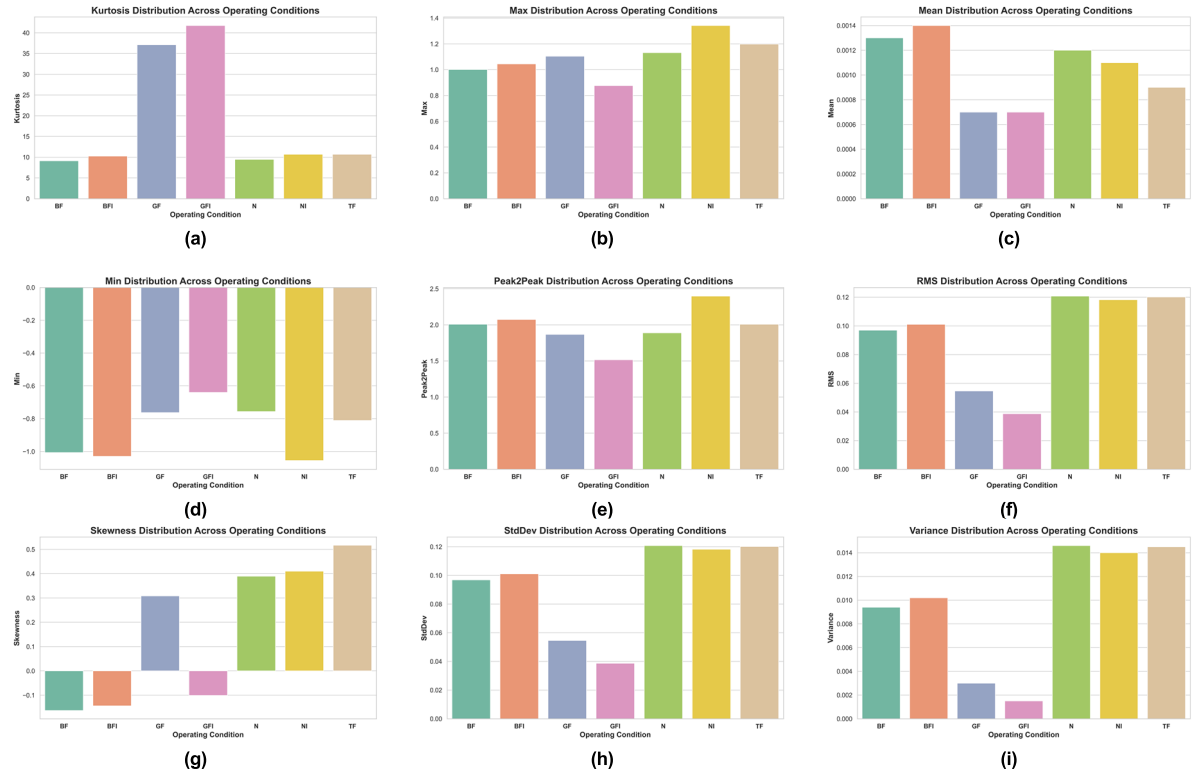

FIGURE 10. Feature-wise bar plots depict the variation of statistical characteristics of AE signals.

To verify that AE signals differ across fault conditions, we extracted key statistical features and visualized them in Figure 10. GFI shows extreme impulsiveness kurtosis $\approx$ 41.75, GF has low signal energy variance ≈ 0.003, NI exhibits the highest amplitude swing peak-to-peak ≈ 2.39, and TF displays strong asymmetry of skewness ≈ 0.52. N, BF, and BFI also demonstrate distinct combinations of RMS, Min, and Max values. These differences reflect physical variations in AE signal behavior across all classes. Such statistical evidence supports the fact that, while visual distinctions in time-frequency plots may not be visible, the underlying signal distributions are learnable by CNNs, enabling robust and accurate classification.

To facilitate effective fault analysis, signals were sampled during both idle and cutting conditions and repeated multiple times for consistency. Specific scenarios were sampled at 25600 Hz using sensors with 100 mV/g sensitivity for the motor and 500 mV/g sensitivity for the chuck. This detailed

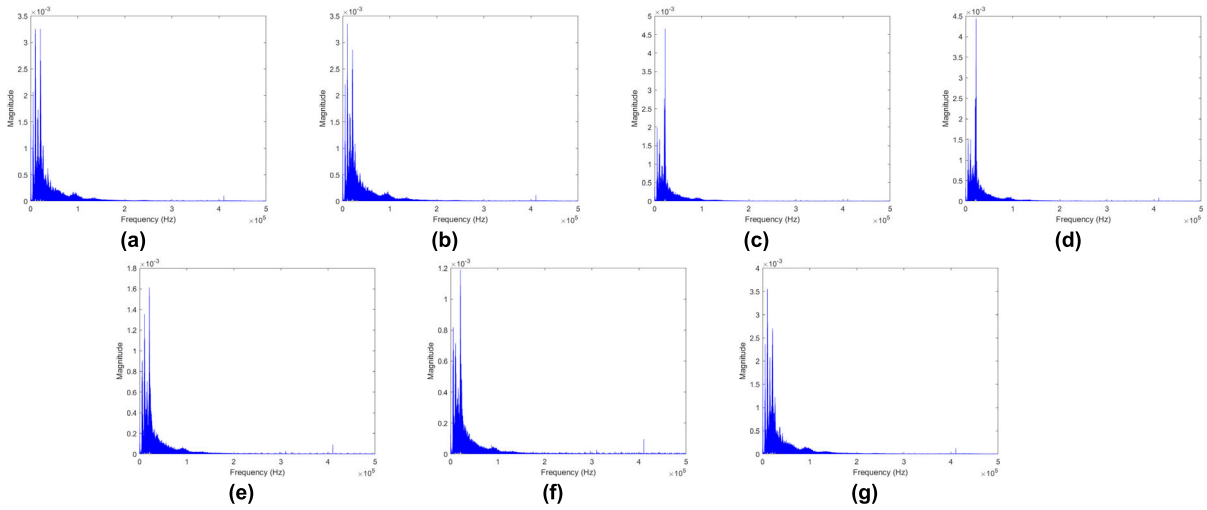

FIGURE 11. AE frequency domain signals: (a) N; (b) NI; (c) BF; (d) BFI; (e) GF; (f) GFI; and (g) TF.

dataset supports robust training and evaluation of models for fault diagnosis in milling operations, ensuring comprehensive coverage of fault scenarios and signal characteristics. Table 6 provides an overview of the operating conditions, detailing the motor speed, spindle speed, and other parameters under normal and faulty scenarios.

B. PERFORMANCE METRICS FOR COMPARISONS

The primary objective of this study was to develop an advanced framework for fault diagnosis in milling machines using AE signals. By utilizing hybrid techniques that integrate time-frequency domain representations, transfer, and dimensionality reduction, this work aimed to overcome the challenges of traditional fault classification methods. To ensure a fair evaluation of the model's performance, the dataset is divided into 80% training data and 20% testing data. Within the training data, the data is further split into 80% for model training and 20% for testing, which is used for hyperparameter tuning and preventing overfitting. Key metrics, namely accuracy, precision, recall, and F1-score, are calculated for the proposed and the comparison models. The mathematical expressions for these metrics are detailed below from equations (1)-(4).

$$\text{Accuracy}\frac{(\text{TP}+\text{TN})}{(\text{TP}+\text{TN}+\text{FP}+\text{FN})}\times 100\% \tag{1}$$

$$\text{Precision} = \frac{\text{TP}}{(\text{TP}+\text{FP})}\times 100\% \tag{2}$$

$$\text{Recall} = \frac{\text{TP}}{(\text{TP}+\text{FN})}\times 100 \tag{3}$$

$$\text{F}_1-\text{Score} = 2\times\frac{\text{Precision}\times\text{Recall}}{\text{Precission}+\text{Recall}} \tag{4}$$

True Positives (TP) refer to instances where the model correctly identifies faulty conditions, while True Negatives (TN) represent cases where non-faulty conditions are accurately classified. False Positives (FP) occur when non-faulty instances are incorrectly classified as faulty, and False Negatives (FN) arise when the model fails to detect faulty conditions, classifying them as non-faulty. Together, these metrics offer a thorough assessment of the model's classification capabilities.

C. COMPARATIVE ANALYSIS

To validate its effectiveness, the proposed method was compared with two reference approaches: a deep learning-based model using ResNet50 and DenseNet121 (DL-Method) [31] and a traditional machine learning approach (Trad-ML) [32] based on handcrafted feature extraction followed by classification. This section presents the classification results, discusses comparative performance, and highlights critical observations and practical implications. The performance of the proposed model was evaluated using a comprehensive dataset consisting of seven distinct classes of N, NI, TF, BF, BFI, GF, and GFI. The proposed method achieved exceptional classification performance across all evaluation metrics, with 99.8% F1-score, 99.7% precision, 99.9% recall, and 99.8% accuracy. This signifies perfect identification and classification of all classes, demonstrating the strength and reliability of the proposed hybrid framework. Additionally, the inference time for the proposed method was 0.04 milliseconds per sample, making it highly efficient for real-time applications. In comparison, the DL-Method achieved an F1-score of 97.5, precision of 97.8, recall of 97.3, and accuracy of 97.5%, with an inference time of 0.1 milliseconds per sample. While this performance is commendable, it falls slightly short of the proposed method due to its inability to effectively handle overlapping feature spaces for complex classes. The Trad-ML approach was implemented using handcrafted statistical features extracted from the AE signals. These included time-domain and frequency-domain features. AE signals were segmented, normalized, and processed before feature extraction. Several classifiers were trained and evaluated,

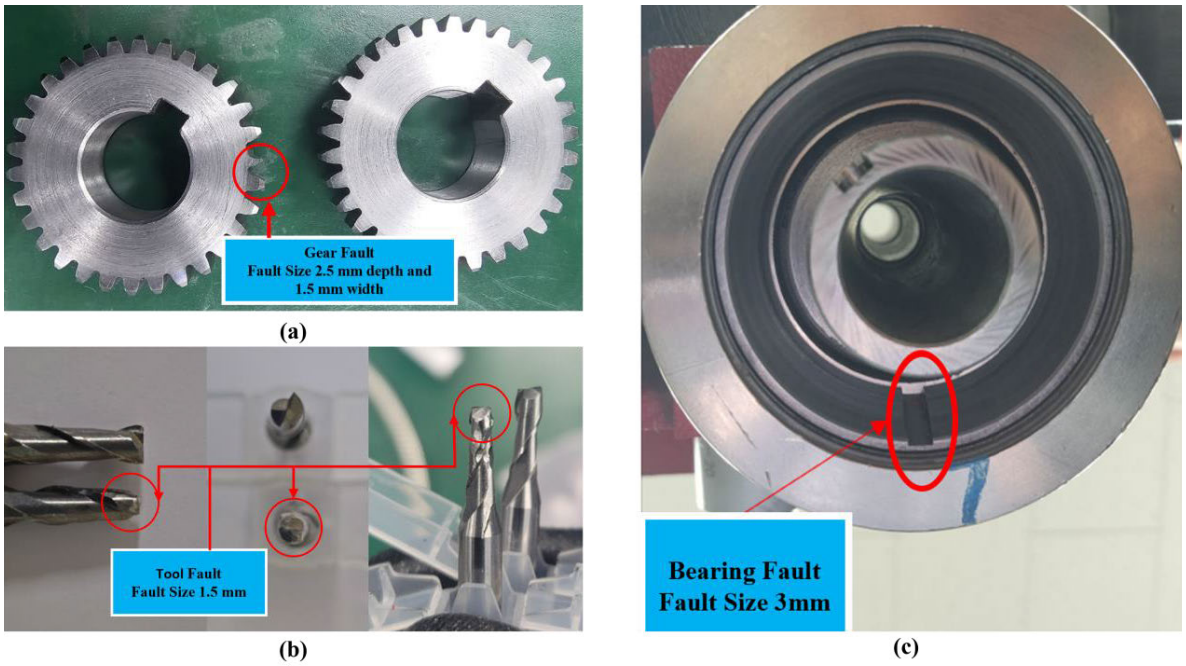

FIGURE 12. Fault components used in the experiment: (a) Gear Fault; (b) Tool Fault; and (c) Bearing Fault.

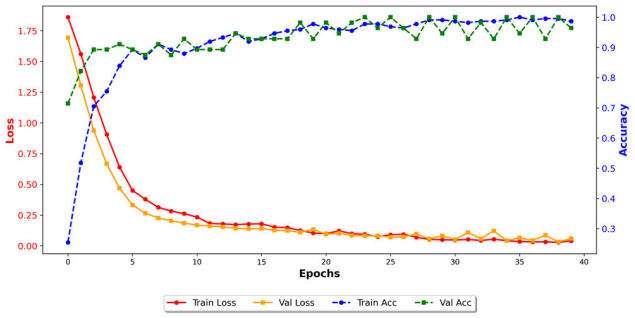

FIGURE 13. Training and validation loss and accuracy curves over epochs.

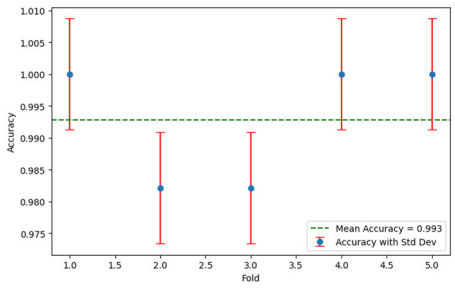

FIGURE 14. 5-fold cross-validation accuracy results.

including Support Vector Machine (SVM), k-Nearest Neighbours (k-NN), Decision Tree (DT), and Random Forest (RF). Hyperparameters for each model were optimized using 5-fold cross-validation. Among them, RF achieved the best performance and was selected as the representative Trad-ML model in the main results. This referenced model performed noticeably worse, achieving an F1-score of 92.8, precision of 92.2, recall of 92.5, and accuracy of 92.8%, with an inference time of 0.09 milliseconds per sample. The lower performance of this method is attributed to its reliance on handcrafted features, which may lack the granularity and discriminative features required for accurate fault classification in complex and noisy datasets. A summary of these results is provided in Table 7 for comparison.

The proposed method performed significantly better than the two reference models across all performance metrics. The DL-Method, while using robust architectures like ResNet50 and DenseNet121, is limited by its inability to fully optimize features across multiple domains. The lack of a dimensionality reduction step, such as in UMAP, further constrains its ability to manage high-dimensional feature spaces, leading to reduced accuracy and increased inference time. To ensure that the proposed model does not suffer from overfitting, we implemented stratified 5-fold cross-validation on the training set. The model achieved an average test accuracy of 99.30% across all folds, with minimal standard deviation, indicating consistent performance and strong generalization. Likewise, the training and validation accuracy curves for the lightweight neural network classifier demonstrate stable learning with minimal signs of overfitting, further confirming the model's robustness and generalization ability, as shown in Figure 13. Similarly, Figure 14 presents the cross-validation results, where each fold maintains high accuracy with negligible variation.

Additionally, to further validate generalizability, the model was evaluated on a completely separate test dataset that was not used during training or testing. On the other hand, the Trad-ML approach, which depends on manually engineered

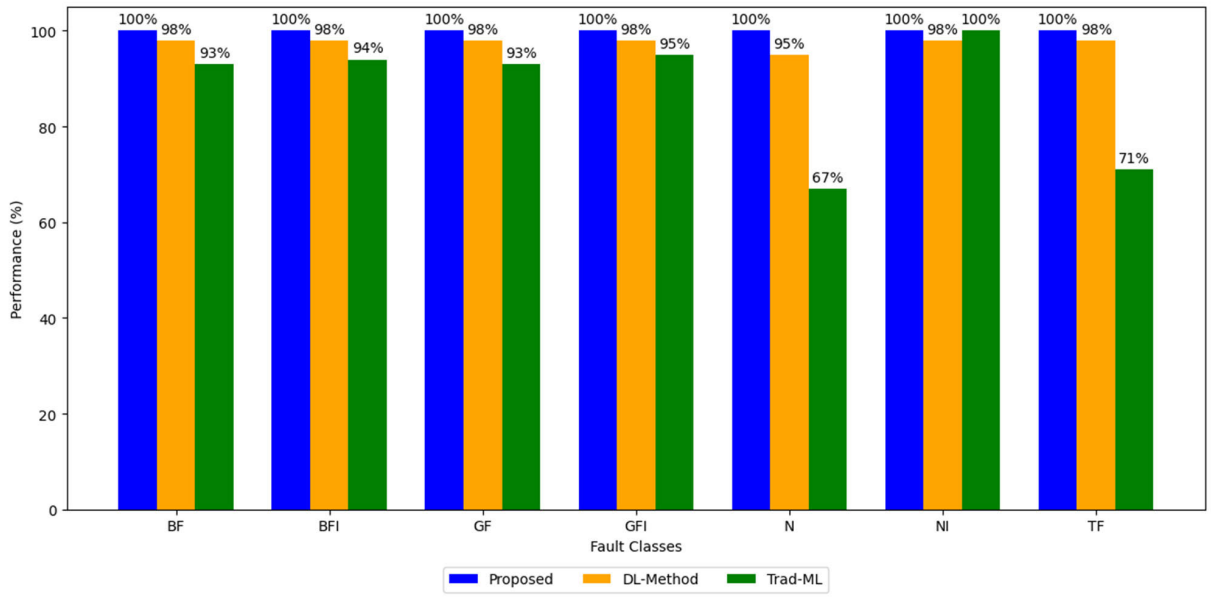

FIGURE 15. Performance comparison chart for each class of the milling machine.

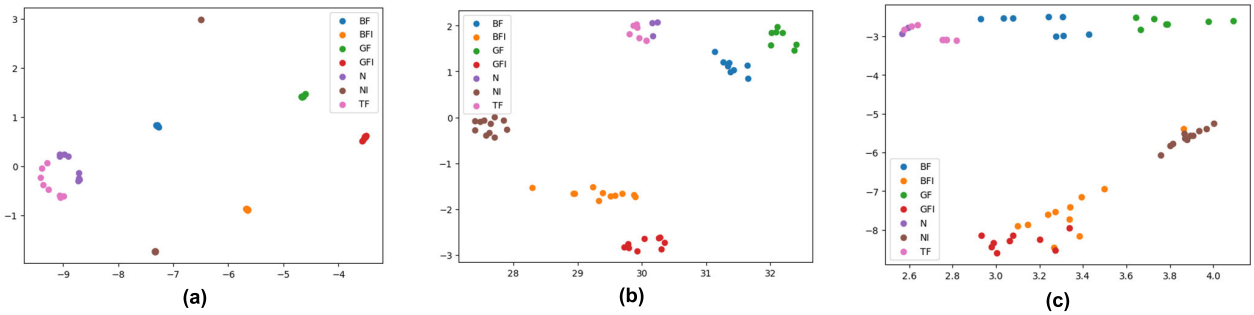

FIGURE 16. Visualization of t-SNE plots: (a) The proposed model; (b) DL-Method; (c) Trad-ML.

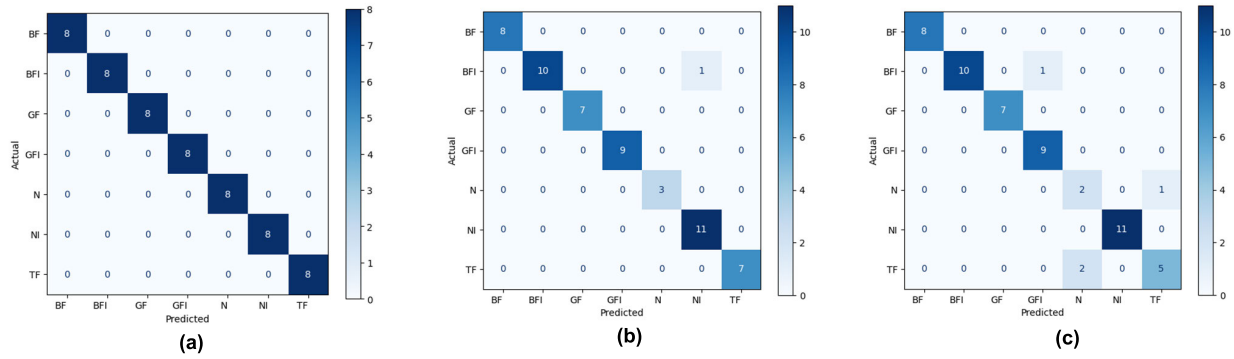

FIGURE 17. Visualization of confusion matrices: (a) The proposed model; (b) DL-Method; (c) Trad-ML.

features, struggles with capturing the complex, non-linear patterns present in AE signals, resulting in lower classification performance. The better performance of the proposed method can be attributed to its hybrid framework, which combines CWT scalograms and STFT spectrograms for comprehensive time-frequency analysis. Using pre-trained architectures for feature extraction and UMAP for dimensionality reduction, the proposed method ensures the retention of important information while minimizing redundancy. The use of k-NN for classification further enhances its performance, offering a simple yet effective approach for distinguishing between all classes.

The performance comparison across all classes is visualized in Figure 15, highlighting the better classification capabilities of the proposed method than the two reference models. The proposed method achieved better classification

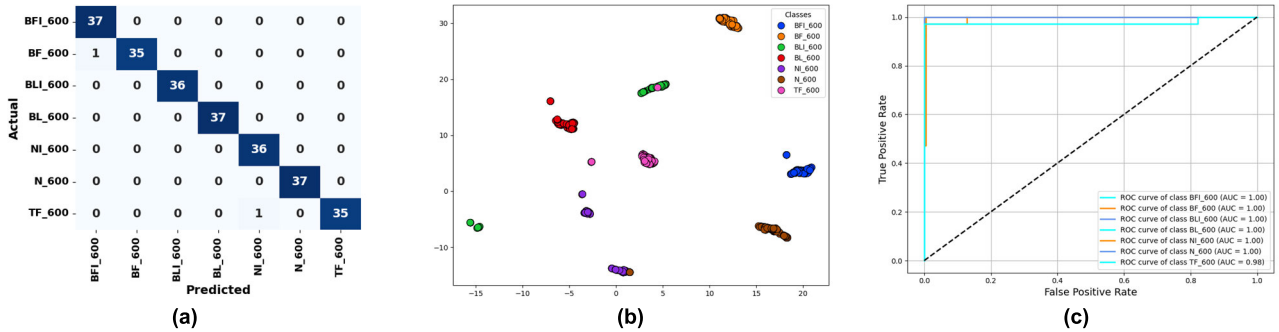

FIGURE 18. Performance evaluation of proposed method on expanded Milling data: (a) Confusion matrix; (b) t-SNE visualization; (c) ROC curve.

TABLE 7. Performance comparison of the proposed method.

Model	Accuracy	Precision	Recall	F1-Score	Inference Time (ms/sample)
Proposed	99.8	99.7	99.9	99.8	0.04
DL-Method	97.5	97.8	97.3	97.5	0.10
Trad-ML	92.8	92.2	92.5	92.8	0.09

performance, with better accuracy, F1-score, precision, and recall across all operating conditions classes, as evident from the uniformly high bars for each fault condition. Furthermore, all the experiments of the proposed model as well as comparison models, are carried out using a Windows 10 system with an Intel 64 Family 6 CPU, NVIDIA GeForce GTX 1050 GPU, and 32GB RAM. The model was implemented using Python 3.12.5. These results demonstrate the robustness and reliability of the method in handling complex and overlapping features in acoustic emission signals. The consistent performance of the proposed method underscores its scalability and applicability for real-time industrial fault detection.

To illustrate the effectiveness of the proposed method, t-SNE plots and confusion matrices were generated. The t-SNE plot for the proposed method in Figure 16 shows clear and distinct clusters for each category, indicating excellent separability and minimal overlap. This highlights the ability of the proposed method to effectively capture and represent discriminative features in a reduced-dimensional space. In contrast, the t-SNE plots for the DL-Method and Trad-ML approaches reveal significant class overlap, particularly for closely related fault types. This overlap indicates that these methods struggle to separate all operating conditions characteristics, leading to misclassifications. The confusion matrix for the proposed method, as shown in Figure 17, shows no misclassification, with all samples correctly identified across all classes. In comparison, the confusion matrices for the DL-Method and Trad-ML approaches reveal several misclassifications, particularly for fault classes with overlapping features, further emphasizing the superiority of the proposed method.

To evaluate the generalization capability of the proposed method on a larger dataset, additional experiments were conducted using an expanded version of the Milling Machine dataset. This dataset retains the same seven classes summarized in Table 5, representing various operational conditions; however, the number of samples per class has been increased to 182, resulting in a total of 1,274 samples. The data acquisition protocol, including sensor placement, sampling frequency, machine configuration, and fault types, was kept strictly consistent with the original experimental setup described in Section III. A (Experimental Setup and Data Acquisition) to ensure a fair and reliable validation environment. The proposed method was applied without any modifications to the model architecture and achieved an average accuracy exceeding 99%, with precision, recall, and F1-score all greater than 95%. These results validate the strong generalization capability of the model across varying sample sizes. Further evidence of the model's robustness and reliability is provided in Figure 18, which presents the confusion matrix, t-SNE visualization, and ROC curves for all classes.

The success of the proposed method can be attributed to several key factors. First, the combination of both CWT and STFT is utilized in a complementary fashion to capture the localized transient bursts and global spectral trends of acoustic emission signals. While CWT offers superior adaptability through adjustable wavelet functions, STFT still contributes valuable fixed-resolution features that reflect quasi-stationary patterns. This dual representation enriches the feature space, improving robustness and generalization, especially under data-limited conditions. Second, the use of transfer learning enables the extraction of powerful, high-level features from the scalograms and spectrograms. Third, the application of UMAP for dimensionality reduction addresses the challenges associated with high-dimensional data, ensuring computational efficiency without compromising feature integrity. By reducing the dimensionality of the feature space, UMAP enhances the performance, enabling accurate and efficient classification. Last, the simplicity and strength of the k-NN algorithm ensure that the proposed method is accurate

and computationally efficient, making it suitable for real-time applications. The proposed method offers significant potential for real-world applications in milling machine fault diagnosis. Its high accuracy and low inference time make it well-suited for real-time monitoring and predictive maintenance, enabling manufacturers to detect and address faults before they lead to machine downtime or costly repairs. Furthermore, the scalability of the proposed framework ensures its applicability to other industrial systems, providing a versatile solution for fault diagnosis across various domains.

IV. CONCLUSION

This study presents a robust and efficient framework for fault diagnosis in milling machines by combining advanced signal processing, transfer learning, and dimensionality reduction techniques. By transforming acoustic emission signals into time-frequency representations, namely continuous wavelet transforms, scalograms, and short-time Fourier transform spectrograms, the proposed method captures localized and transient signal patterns essential for accurate fault trained on large datasets, and discriminative high-level features are extracted. Dimensionality reduction using uniform manifold approximation and projection ensures computational efficiency while maintaining feature integrity, enabling real-time applications. Integrating UMAP-reduced features with a k-Nearest Neighbours classifier resulted in outstanding classification accuracy, achieving a cross-validation accuracy of 99.6%. The results highlight the method's ability to address challenges associated with the transient and non-stationary nature of AE signals. Finally, to evaluate the individual contributions of CWT and STFT, we conducted an ablation study using identical classification pipelines. The results indicate that CWT-only features achieved 93.43% accuracy while STFT-only features with 90.71% accuracy.

Future research will focus on extending this approach to larger and more diverse datasets to validate its generalizability. Additionally, exploring the current study on different machining conditions, as well as integrating the framework with advanced monitoring systems, may further enhance its application for fault diagnosis and predictive maintenance.

REFERENCES

[1] A. Przybyś-Małaczek, I. Antoniuk, K. Szymanowski, M. Kruk, and J. Kurek, "Application of machine learning algorithms for tool condition monitoring in milling chipboard process," *Sensors*, vol. 23, no. 13, p. 5850, Jun. 2023, doi: 10.3390/s23135850.

[2] D. Kaliyannan, M. Thangamuthu, P. Pradeep, S. Gnansekaran, J. Rakkiyannan, and A. Pramanik, "Tool condition monitoring in the milling process using deep learning and reinforcement learning," *J. Sensor Actuator Netw.*, vol. 13, no. 4, p. 42, Jul. 2024, doi: 10.3390/jsan13040042.

[3] D. Bourassa, F. Gauthier, and G. Abdul-Nour, "Equipment failures and their contribution to industrial incidents and accidents in the manufacturing industry," *Int. J. Occupational Saf. Ergonom.*, vol. 22, no. 1, pp. 131–141, Jan. 2016, doi: 10.1080/10803548.2015.1116814.

[4] M. Ingale, R. Bhortake, and K. Waghulde, "A comparative study of measurement systems using machine learning techniques for tool fault di-agnosis during metal removal in the milling process," *J. Mines, Met. Fuels*, vol. 2024, pp. 987–1004, Oct. 2024, doi: 10.18311/jmmf/2024/45398.

[5] T. Mohanraj, E. S. Kirubakaran, D. K. Madheswaran, M. L. Naren, and M. Ibrahim, "Review of advances in tool condition monitoring techniques in the milling process," *Meas. Sci. Technol.*, vol. 35, no. 9, Sep. 2024, Art. no. 092002, doi: 10.1088/1361-6501/ad519b.

[6] M. Ragnoli, M. Pavone, N. Epicoco, G. Pola, E. De Santis, G. Barile, and V. Stornelli, "A condition and fault prevention monitoring system for industrial computer numerical control machinery," *IEEE Access*, vol. 12, pp. 20919–20930, 2024, doi: 10.1109/ACCESS.2024.3359424.

[7] A. Rani, D. Ortiz-Arroyo, and P. Durdevic, "A survey of vision-based condition monitoring methods using deep learning: A synthetic fiber rope perspective," *Eng. Appl. Artif. Intell.*, vol. 136, Oct. 2024, Art. no. 108921, doi: 10.1016/j.engappai.2024.108921.

[8] N. W. Nirwan and H. B. Ramani, "Condition monitoring and fault detection in roller bearing used in rolling mill by acoustic emission and vibration analysis," *Mater. Today, Proc.*, vol. 51, pp. 344–354, Jan. 2022, doi: 10.1016/j.matpr.2021.05.447.

[9] Q. Liu, J. Liu, X. Liu, J. Ma, and B. Zhang, "Based on domain adversarial neural network with multiple loss collaborative optimization for milling tool wear state monitoring under different machining conditions," *Precis. Eng.*, vol. 91, pp. 692–706, Dec. 2024, doi: 10.1016/j.precisioneng.2024.11.005.

[10] J. Liu, C. Jiang, H. Jiang, and Z. Jiang, "Optimizing tool life in SiCp/Al composites milling with acoustic emission analysis: A comprehensive monitoring and implementation strategy," *J. Manuf. Processes*, vol. 120, pp. 920–928, Jun. 2024, doi: 10.1016/j.jmapro.2024.05.009.

[11] L. Li, H. Liu, H. Xie, T. Zhang, H. Tian, S. Zhang, J. Cai, L. Sun, X. Liu, H. Cao, T. Liu, and Z. Jiang, "Finite element analysis of strip shape regulation ability of work roll shifting in a 4-high hot strip mill," *J. Manuf. Processes*, vol. 131, pp. 1642–1655, Dec. 2024, doi: 10.1016/j.jmapro.2024.09.106.

[12] L. Senjoba, H. Ikeda, H. Toriya, T. Adachi, and Y. Kawamura, "Enhancing interpretability in drill bit wear analysis through explainable artificial intelligence: A grad-CAM approach," *Appl. Sci.*, vol. 14, no. 9, p. 3621, Apr. 2024, doi: 10.3390/app14093621.

[13] Y. Yuan, J. Wei, H. Huang, W. Jiao, J. Wang, and H. Chen, "Review of resampling techniques for the treatment of imbalanced industrial data classification in equipment condition monitoring," *Eng. Appl. Artif. Intell.*, vol. 126, Nov. 2023, Art. no. 106911, doi: 10.1016/j.engappai.2023.106911.

[14] K. Barrera-Llanga, J. Burriel-Valencia, Á. Sapena-Bañó, and J. Martínez-Román, "A comparative analysis of deep learning convolutional neural network architectures for fault diagnosis of broken rotor bars in induction motors," *Sensors*, vol. 23, no. 19, p. 8196, Sep. 2023, doi: 10.3390/s23198196.

[15] J.-H. Han, D.-J. Choi, S.-K. Hong, and H. Kim, "Motor fault diagnosis using CNN based deep learning algorithm considering motor rotating speed," in *Proc. IEEE 6th Int. Conf. Ind. Eng. Appl. (ICIEA)*, Apr. 2019, pp. 440–445, doi: 10.1109/IEA.2019.8714900.

[16] I. D. López, J. F. Grass, A. Figueroa, and J. C. Corrales, "A proposal for a multi-domain data fusion strategy in a climate-smart agriculture context," *Int. Trans. Oper. Res.*, vol. 30, no. 4, pp. 2049–2070, Jul. 2023, doi: 10.1111/itor.12899.

[17] Y. Li and D. A. Ramli, "Advances in time-frequency analysis for blind source separation: Challenges, contributions, and emerging trends," *IEEE Access*, vol. 11, pp. 137450–137474, 2023, doi: 10.1109/ACCESS.2023.3338024.

[18] E. Paolini, L. Valcarenghi, L. Maggiani, and N. Andriolli, "Real-time network packet classification exploiting computer vision architectures," *IEEE Open J. Commun. Soc.*, vol. 5, pp. 1155–1166, 2024, doi: 10.1109/OJCOMS.2024.3363082.

[19] M. Boyer, L. Bouyer, J.-S. Roy, and A. Campeau-Lecours, "Reducing noise, artifacts and interference in single-channel EMG signals: A review," *Sensors*, vol. 23, no. 6, p. 2927, Mar. 2023, doi: 10.3390/s23062927.

[20] S. Sayyad, S. Kumar, A. Bongale, P. Kamat, S. Patil, and K. Kotecha, "Data-driven remaining useful life estimation for milling process: Sensors, algorithms, datasets, and future directions," *IEEE Access*, vol. 9, pp. 110255–110286, 2021, doi: 10.1109/ACCESS.2021.3101284.

[21] P. Twardowski, M. Tabaszewski, M. Wiciak-Pikula, and A. Felusiak-Czyryca, "Identification of tool wear using acoustic emission signal and machine learning methods," *Precis. Eng.*, vol. 72, pp. 738–744, Nov. 2021, doi: 10.1016/j.precisioneng.2021.07.019.

[22] R. Medina, R.-V. Sánchez, D. Cabrera, M. Cerrada, E. Estupiñan, W. Ao, and R. E. Vásquez, "Gearbox faults severity classification using poincaré plots of acoustic emission signals," *Appl. Acoust.*, vol. 219, Mar. 2024, Art. no. 109918, doi: 10.1016/j.apacoust.2024.109918.
[23] D. Li, H. Gao, K. Yang, F. Zhou, and X. Shi, "Abnormal identification of oil monitoring based on LSTM and SVDD," *Wear*, vols. 526–527, Aug. 2023, Art. no. 204793, doi: 10.1016/j.wear.2023.204793.
[24] X. Bai, "Fault diagnosis technology of CNC electromechanical system in mechanical engineering equipment manufacturing under structural coupling," *Appl. Math. Nonlinear Sci.*, vol. 9, no. 1, pp. 1–16, Jan. 2024, doi: 10.2478/amns-2024-0688.
[25] L. Wang and J. Xiang, "A two-stage method using spline-kernelled chirplet transform and angle synchronous averaging to detect faults at variable speed," *IEEE Access*, vol. 7, pp. 22471–22485, 2019, doi: 10.1109/ACCESS.2019.2898884.
[26] R. Zaheer, I. Ahmad, D. Habibi, K. Y. Islam, and Q. V. Phung, "A survey on artificial intelligence-based acoustic source identification," *IEEE Access*, vol. 11, pp. 60078–60108, 2023, doi: 10.1109/ACCESS.2023.3283982.
[27] A. S. Alhanaf, M. Farsadi, and H. H. Balik, "Fault detection and classification in ring power system with DG penetration using hybrid CNN-LSTM," *IEEE Access*, vol. 12, pp. 59953–59975, 2024, doi: 10.1109/ACCESS.2024.3394166.
[28] G. Chen, J. Yuan, Y. Zhang, H. Zhu, R. Huang, F. Wang, and W. Li, "Enhancing reliability through interpretability: A comprehensive survey of interpretable intelligent fault diagnosis in rotating machinery," *IEEE Access*, vol. 12, pp. 103348–103379, 2024, doi: 10.1109/ACCESS.2024.3430010.
[29] M. F. Siddique, Z. Ahmad, N. Ullah, and J. Kim, "A hybrid deep learning approach: Integrating short-time Fourier transform and continuous wavelet transform for improved pipeline leak detection," *Sensors*, vol. 23, no. 19, p. 8079, Sep. 2023, doi: 10.3390/s23198079.
[30] M. F. Siddique, W. Zaman, S. Ullah, M. Umar, F. Saleem, D. Shon, T. H. Yoon, D.-S. Yoo, and J.-M. Kim, "Advanced bearing-fault diagnosis and classification using mel-scalograms and FOX-optimized ANN," *Sensors*, vol. 24, no. 22, p. 7303, Nov. 2024, doi: 10.3390/s24227303.
[31] Y. Zheng, B. Chen, B. Liu, and C. Peng, "Milling cutter wear state identification method based on improved ResNet-34 algorithm," *Appl. Sci.*, vol. 14, no. 19, p. 8951, Oct. 2024, doi: 10.3390/app14198951.
[32] A. D. Patange and R. Jegadeeshwaran, "Review on tool condition classification in milling: A machine learning approach," *Mater. Today, Proc.*, vol. 46, pp. 1106–1115, Jan. 2021, doi: 10.1016/j.matpr.2021.01.523.

MUHAMMAD UMAR received the bachelor's degree in computer systems engineering from the University of Engineering and Technology (UET), Peshawar, Pakistan, in 2023. He is currently pursuing the degree in artificial intelligence and computer engineering with the University of Ulsan, South Korea. In March 2024, he joined Ulsan Industrial Artificial Intelligence (UIAI) Laboratory, as a Research Student. His research interests include artificial intelligence, deep learning, signal processing, and data-driven methods for fault diagnosis and prognosis.

ZAHOOR AHMAD received the B.S. degree in computer engineering from the COMSATS Institute of Information Technology (CIIT), now known as COMSATS University Islamabad (CUI), Attock, Pakistan, in 2016, the M.S. degree in electronics and information engineering from Korea Aerospace University (KAU), Goyang-si, South Korea, in 2019, and the Ph.D. degree from the University of Ulsan, South Korea. Since 2023, he has been a Postdoctoral Research Fellow with Ulsan Industrial Artificial Intelligence (UIAI) Laboratory, University of Ulsan. His current research interests include artificial intelligence, signal processing, fault diagnosis, condition monitoring of industrial machinery, and fault feature extraction.

SAIF ULLAH received the bachelor's degree in mechatronics engineering and the M.S. degree in electrical control system engineering from the National University of Sciences and Technology (NUST), Islamabad, Pakistan, in 2019 and 2023, respectively. He is currently pursuing the Ph.D. degree in artificial intelligence and computer engineering with the University of Ulsan, South Korea. His research interests include fault diagnosis, condition monitoring, electric vehicles, automation, machine learning, and signal processing.

FAISAL SALEEM received the bachelor's degree in telecommunication engineering from the University of Engineering and Technology, Peshawar, Pakistan, in 2021. He is currently pursuing the combined M.S.-Ph.D. degree in artificial intelligence and computer engineering with the University of Ulsan, South Korea. Since March 2024, he has been a Research Student with Ulsan Industrial Artificial Intelligence (UIAI) Laboratory. His research interests include artificial intelligence, deep learning, signal processing, and fault diagnosis. His current work emphasizes the advancement of intelligent systems for industrial machinery monitoring and vibration-based condition monitoring.

MUHAMMAD FAROOQ SIDDIQUE received the B.S. degree in mechanical engineering from the National University of Science and Technology (NUST), Islamabad, Pakistan, in 2017, and the M.S. degree in mechanical engineering from the University of Engineering and Technology, Peshawar, Pakistan, in 2021. He is currently pursuing the Ph.D. degree with the University of Ulsan under the President's Excellence Scholarship. He is a Graduate Research Assistant with Ulsan Industrial Artificial Intelligence (UIAI) Laboratory, specializing in IT fault diagnosis. His research interests include artificial intelligence, signal processing, fault diagnosis, and vibration-based condition monitoring of industrial machinery.

JONG-MYON KIM (Member, IEEE) received the B.S. degree in electrical engineering from Myongji University, Yongin, South Korea, in 1995, the M.S. degree in electrical and computer engineering from the University of Florida, Gainesville, FL, USA, in 2000, and the Ph.D. degree in electrical and computer engineering from Georgia Institute of Technology, Atlanta, GA, USA, in 2005.

He is currently a Professor with the School of IT Convergence, University of Ulsan, Ulsan, South Korea. His research interests include fault diagnosis and condition monitoring, multimedia-specific processor architecture, parallel processing, and embedded systems. He is a member of the IEEE Industrial Electronics Society.